Supplemental Information

Table S1: Diffraction data and crystallographic refinement statistical values

Structure	CaMKII kinase domain /*d*EAG$_{long}$/ Mg^{2+}-ADP	CaMKII kinase domain /*d*EAG$_{long}$/ Mg^{2+}-AMPPN	CaMKII^{D136N} kinase domain /*d*EAG$^{P}_{long}$/ Mg^{2+}-ADP
PDB entry	5FG8	5H9B	5HU3
Diffraction data			
Space group	$P12_11$	$P12_11$	$P12_11$
Unit cell parameters a, b, c (Å), $\alpha=\gamma$, β	36.50, 59.22, 70.76, 90.00, 97.23	35.82, 59.13, 70.34, 90.00, 99.02	36.91, 59.22, 70.30, 90.00, 96.68
Wavelength (Å)	0.98403	0.98406	0.97625
Resolution range (Å)	30.19-1.88 (1.95-1.88)	45.03-2.25 (2.33-2.25)	30.08-1.82 (1.88-1.82)
No. of unique reflections	23,764 (2,099)	13,806 (1,342)	26,540 (2,412)
No. of measured reflections	77,000 (5,111)	47,277 (4,686)	87,981 (5,854)
Multiplicity	3.2 (2.4)	3.4 (3.5)	3.3 (2.4)
Completeness (%)	97.2 (88.0)	99.4 (99.5)	97.9 (91.0)
I/σI	12.4 (1.5)	10.4 (1.7)	19.3 (1.5)
R_{meas} (%)	6.0 (86.2)	8.0 (93.9)	4.1 (73.6)
Refinement data			
Resolution range (Å)	30.19-1.96 (2.04-1.96)	45.03-2.25 (2.42-2.25)	30.08-1.89 (1.96-1.89)
No. of reflections	21,328	13,780	24,034
R_{work}/R_{free} (%)	19.1/22.1 (29.9/30.3)	20.3/22.2 (32.2/37.8)	19.2/22.8 (39.7/42.0)
No. of atoms in model:			
Protein	2,304	2,288	2,271
Solvent	69	22	79
Nucleotide	27	27	27
Mg^{2+}	1	1	1
Average B value (Å^2):			
Protein	58	76	49
Solvent	44	49	41
Nucleotide	43	69	39
Mg^{2+}	46	72	39
RMSD bond length (Å)	0.010	0.004	0.017
RMSD bond angle (°)	1.171	0.758	1.347

RMSD: root-mean-square deviation. High-resolution bin statistics are shown in parentheses.

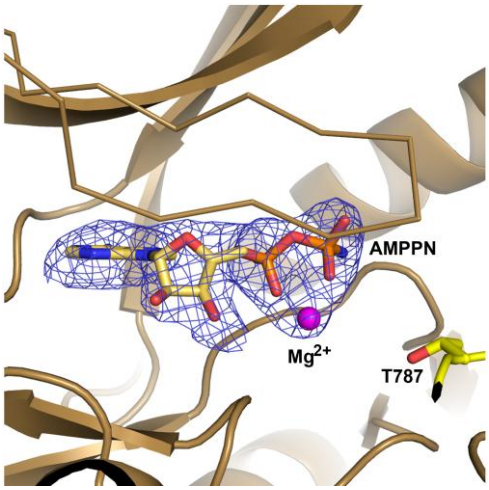

Figure S1: CaMKII kinase domain bound with AMPPN

View of active site of native CaMKII kinase domain (residues 1-283) crystallized in the presence of *d*EAG$_{long}$ and AMPPNP. Mesh shows omit density map revealing the presence of AMPPN. Kinase shown as dark-wheat cartoon and T787 in channel fragment as yellow stick. AMPPN and Mg^{2+} are indicated.

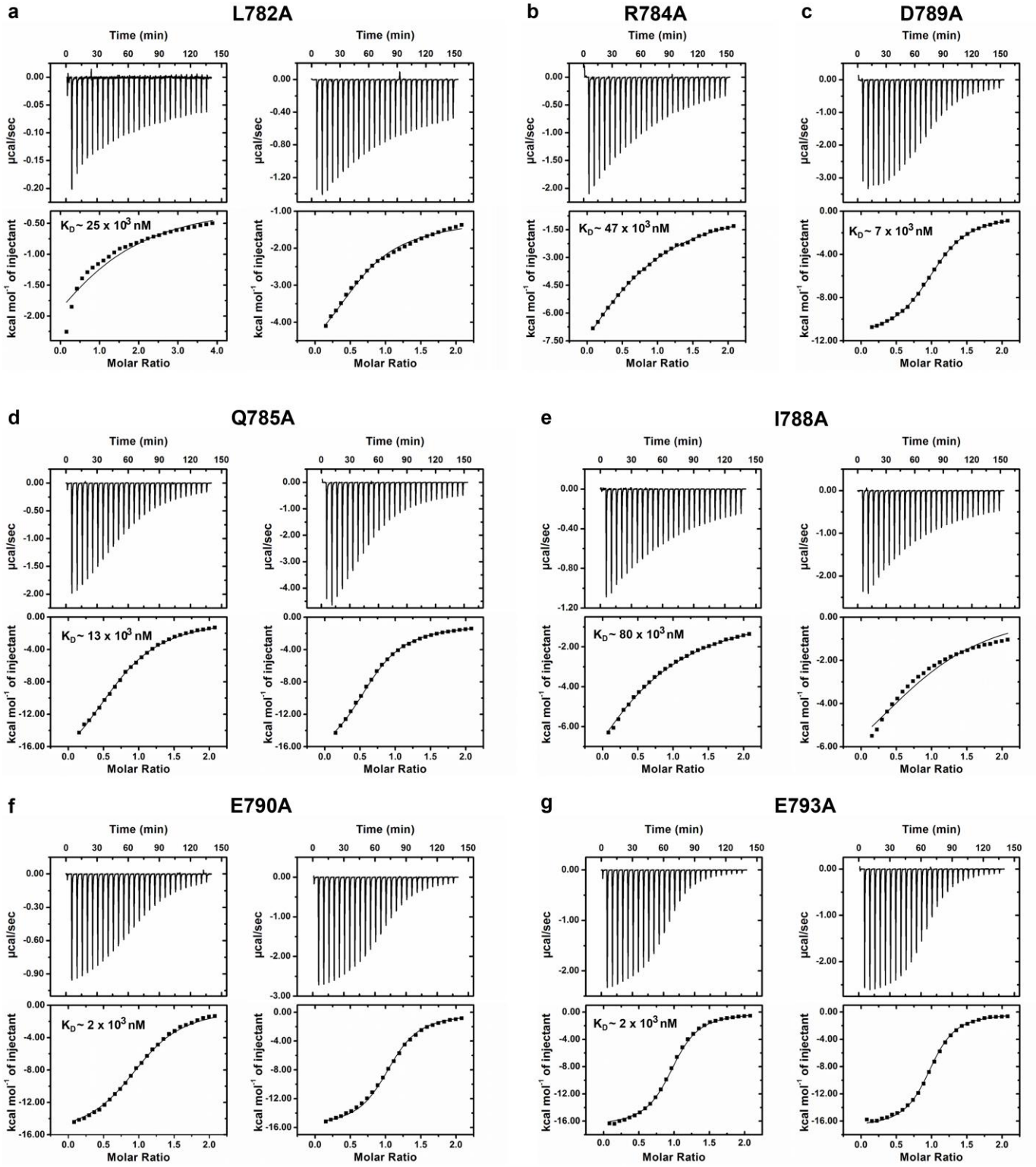

Figure S2: *d*EAG channel fragment alanine scanning experiments.

ITC experiments of wild type CaMKII kinase domain and mutants of *d*EAG$_{long}$ channel fragment in the presence of Mg^{2+}-AMPPNP. Mutants as indicated. Titration injection heats are shown in the upper panel and binding isotherm of integrated binding enthalpies in the lower panel. K_D values are shown for each mutant in lower panels. The large decrease in affinity and/or decrease in protein expression levels for some mutants led us to perform just 2 independent calorimetric assays for L782A, Q785A, I788A, E790A and E793A. In these cases we executed assays at two different

concentrations and performed a global fit of the data using the Affinimeter package. Data and fit for both these experiments is shown. For R784A and D789A one of the three replicas performed is shown.

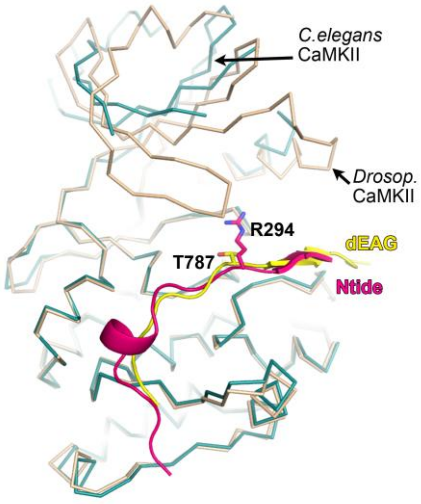

Figure S3: Structural similarity between kinase domain bound to *d*EAG and bound to the CaMKII inhibitor Ntide.

CaMKII kinase domain/*d*EAG$_{long}$ complex (in wheat color) with bound Mg^{2+}-ADP superposed on CaMKII kinase domain/Ntide complex (shown in cyan; PDB entry: 3KL8) from *C. elegans*. Channel fragment (*d*EAG) in yellow and Ntide (Ntide) in magenta. Residues T787 in *d*EAG and R294 in Ntide shown in stick. Superposition matched position of Cα-atoms in the C-lobe of the two kinase domains (residues 97-275).

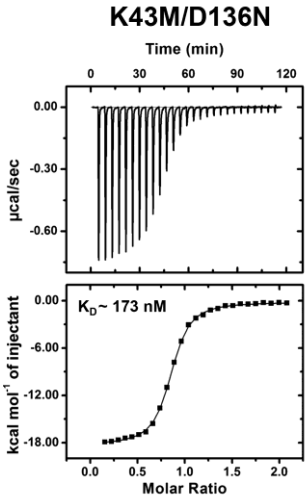

Figure S4: Determination of affinity of channel fragment for CaMKII kinase domain mutant.

ITC experiment of kinase domain K43M/D136N double mutant titrated with *d*EAG$_{short}$ channel fragment in the presence of Mg^{2+}-AMPPNP. Titration injection heats are shown in the upper panel and binding isotherm of integrated binding enthalpies in the lower panel. K_D value is shown in lower panel.

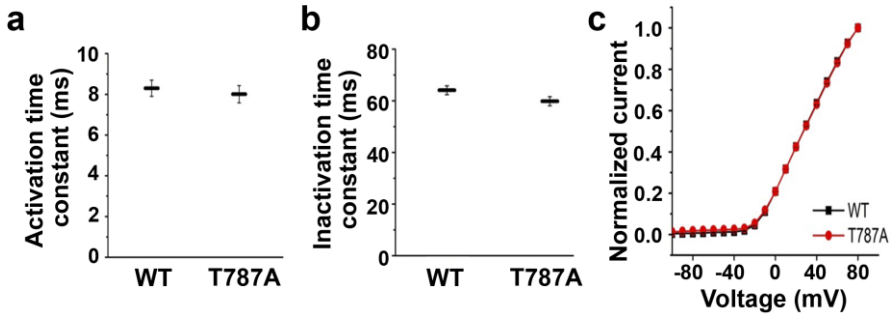

Figure S5: Current characteristics for WT and T787A *d*EAG channels

Comparison of **a)** activation time constant and **b)** inactivation time constant of WT and T787A *d*EAG channel current evoked at 60 mV. **c)** Comparison of the WT and T787A *d*EAG channel current-voltage relationship. Data are mean ± SEM and n=7-8.

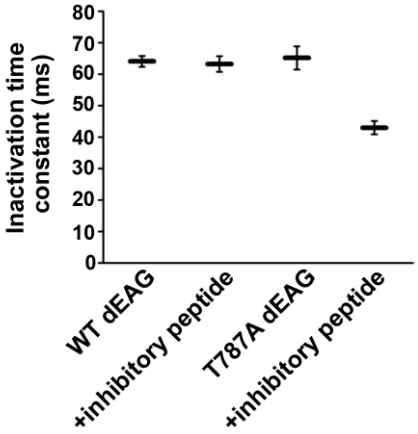

Figure S6: Inactivation time constant for *d*EAG channel

Inactivation time constant of current at 60 mV mediated by WT *d*EAG channel alone and exposed to the inhibitory peptide, T787A *d*EAG channel alone and exposed to the inhibitory peptide. Data are mean ± SEM and n=7-10.

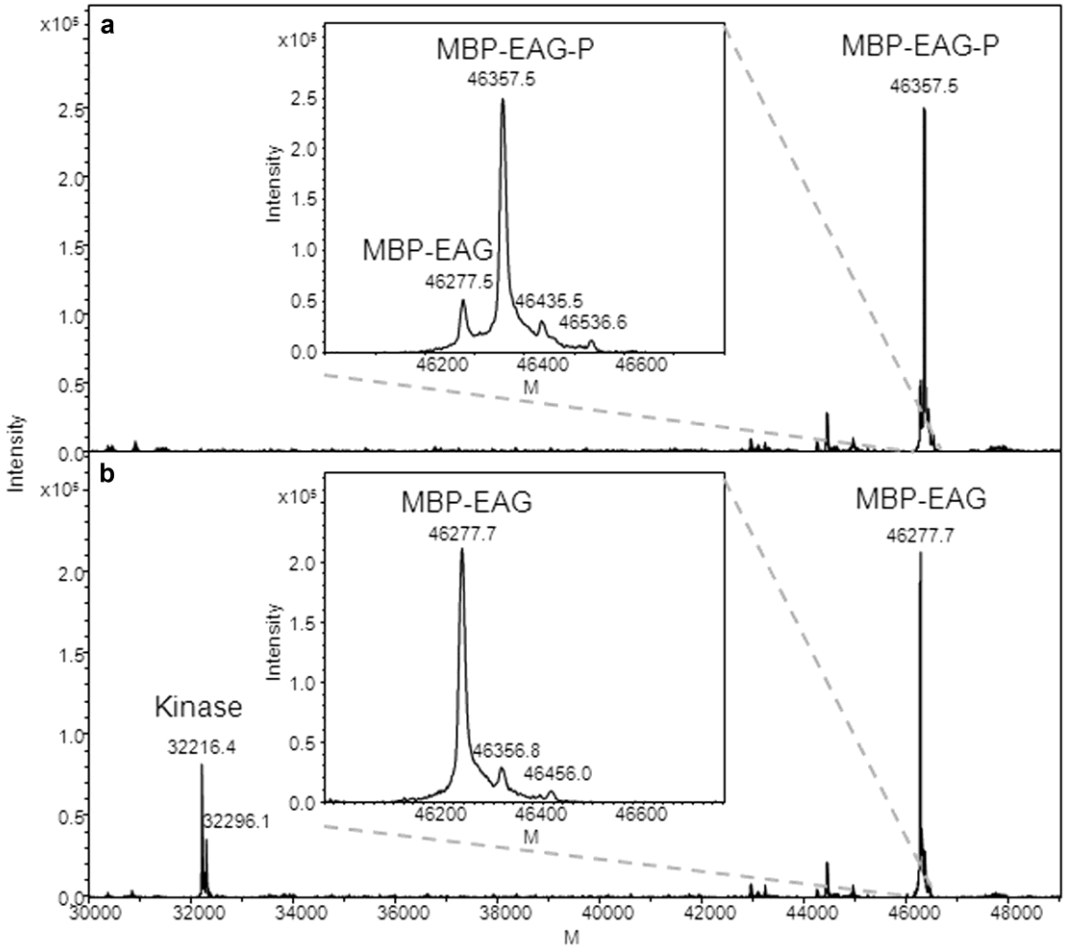

Figure S7: Mass spectrometry spectra of samples before and after ITC experiments showing dephosphorylation.

Deconvoluted UHR-QTOF mass spectra of phosphorylated MBP-*d*EAG$_{short}$ before **a)** and after **b)** ITC experiment in the presence of wild type CaMKII kinase domain and Mg^{2+}-AMPCP.

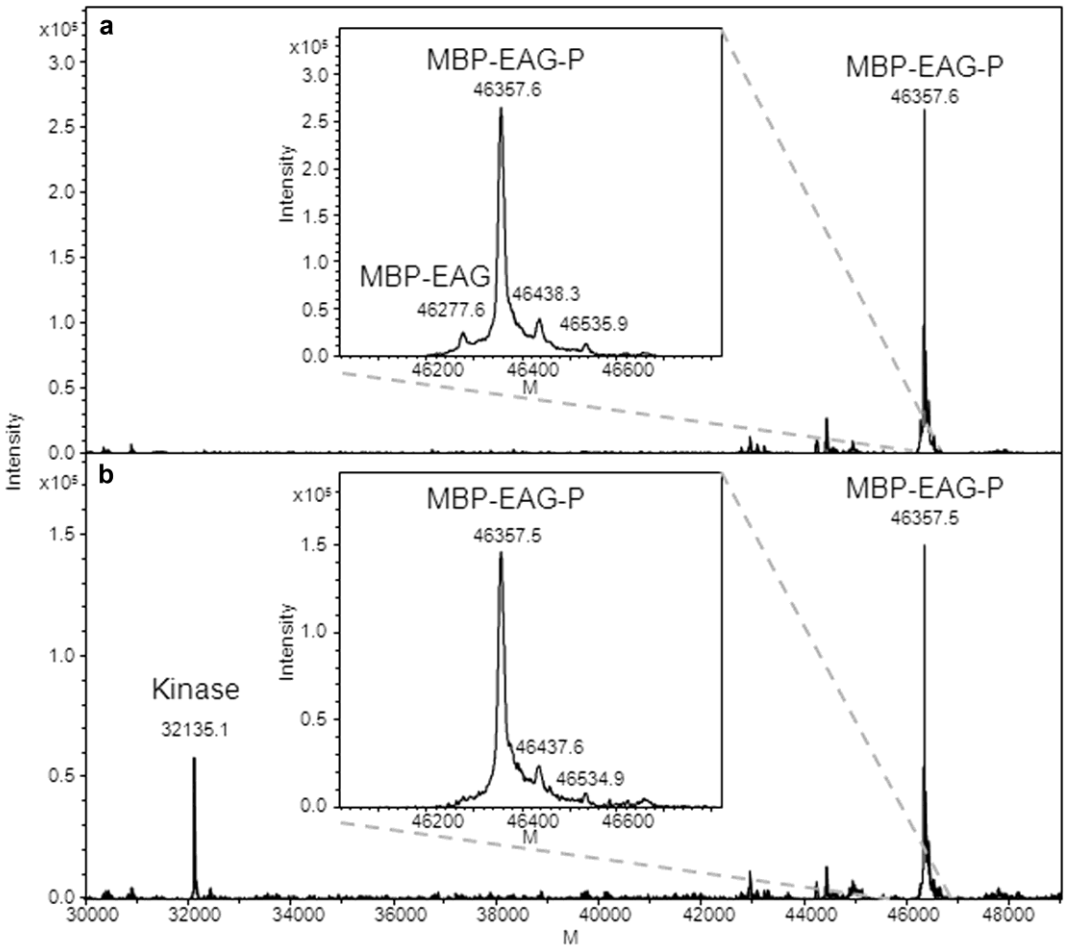

Figure S8: Mass spectrometry spectra of samples before and after ITC experiments showing no change in phosphorylation.

Deconvoluted UHR-QTOF mass spectra of phosphorylated MBP-*d*EAG before **a)** and after **b)** ITC experiment in the presence of D136N CaMKII kinase domain and Mg^{2+}-ADP.